POTENTIAL IMPACTS OF CABLE BACTERIA ACTIVITY ON HARD-SHELLED BENTHIC FORAMINIFERA: IMPLICATIONS FOR THEIR INTERPRETATION AS BIOINDICATORS OR PALEOPROXIES

Maxime Daviray[1]*, Emmanuelle Geslin[1], Nils Risgaard-Petersen[2], Vincent V. Scholz[3], Marie Fouet[1,4], Edouard Metzger[1]

*Correspondence: Maxime DAVIRAY (maxime.daviray@univ-angers.fr)

1. Univ Angers, Nantes Université, Le Mans Université, CNRS, Laboratoire de Planétologie et Géosciences, LPG UMR 6112, 49000 Angers, France
2. Aquatic Biology, Department of Biology, Aarhus University, 8000 Aarhus C, Denmark
3. Center for Electromicrobiology, Department of Biology, Aarhus University, 8000 Aarhus C, Denmark
4. at present: UMR CNRS 5805 EPOC - OASU, Station Marine d'Arcachon, Université de Bordeaux, CNRS, 33120 Arcachon, France

ABSTRACT

Hard-shelled foraminifera are protists able to build a calcareous or agglutinated shell (called "test"). Here we study the impact of sediment acidification on calcareous test preservation. For this study, sediment cores were sampled in the macrotidal Auray estuary located on the French Atlantic coast. Living and dead foraminifera were quantified until 5-cm depth and discriminated using the Cell-Tracker™ Green vital marker. pH and oxygen profiles combined with quantitative Polymerase Chain Reaction (q-PCR) suggested that cable bacteria were most likely to cause the acidifying process. Cable bacteria (CB) are filamentous bacteria coupling sulphide oxidation to oxygen reduction over centimetre distances generating a strong pH gradient within the first few centimetres of the sediment that could affect the microhabitats occupied by benthic foraminifera. On two different intertidal mudflats, volumetric filament densities have been estimated. They were comparable to those observed in the literature for coastal environments, with 7.4 ± 0.4 and 74.4 ± 5.0 $m.cm^{-3}$ per bulk sediment respectively. Highly contrasting sediment acidification (from low to very intense) were described from 1.0 to 2.4 ΔpH. This seems to lead to various dissolution stages of the foraminiferal calcareous test from intact to fully dissolved tests revealing the organic lining. The dissolution scale is based on observations of living *Ammonia* spp. and *Haynesina germanica* specimens under a Scanning Electronic Microscope. Furthermore, dead foraminiferal assemblages showed a strong calcareous test loss and an organic lining accumulation throughout depth under low pH, hampering the test preservation in deep sediment. These changes in both living and dead foraminiferal assemblages suggest that cable bacteria must be considered in ecological monitoring and historical studies using foraminifera as bioindicator and paleoenvironmental proxy.

1 INTRODUCTION

Benthic foraminifera are unicellular meiofaunal organisms. Most species can build a hard-shell (called a test) that can be agglutinated (cemented grains), hyaline calcareous (calcium carbonate) and porcelaneous calcareous (calcium carbonate enriched in magnesium). Benthic foraminifera are very abundant in marine areas (Martin, 2000) including transitional environments (Alve & Murray, 1999; Debenay et al., 2006). These systems located between marine and continental areas (i.e. littoral and estuarine zones), are subjected to a high variability of environmental factors (e. g. tide, freshwater flows, evaporation, development of seagrass meadows over seasonal cycles...). Then, benthic foraminifera are submitted to strong variability of physical and geochemical parameters such as temperature, salinity or pH that they must tolerate. Despite such variability, benthic foraminifera assemblages have been used in transitional environments as bioindicators for biomonitoring ecological state and assemblages and chemical test composition as paleoenvironmental proxies to understand past ecosystems functioning (Martin, 2000; Murray, 2006; Katz et al., 2010; Keul et al., 2017; Durand et al., 2018). However, species with a calcareous test can be affected by sediment acidification and carbonate undersaturation leading to test dissolution (Le Cadre et al., 2003; Bentov et al., 2009; de Nooijer et al., 2009; Haynert et al., 2011, 2014; Kurtarkar et al., 2011; Charrieau et al., 2018b). Even if they are rarely observed *in situ*, few studies have reported signs of severe test dissolution in living assemblages (e.g., Alve and Nagy, 1986; Buzas-Stephens, 2005; Polovodova and Schonfeld, 2008; Haynert et al., 2012; Cesbron et al., 2016; Charrieau et al., 2018a; Schönfeld and Mendes, 2022). These authors attribute these dissolution observations to low pH and undersaturation of the carbonate system, which would be due to abiotic conditions (anthropogenic pollution, freshwater intrusions) or more rarely to biotic ones (degradation of plants). Under laboratory conditions, Le Cadre et al. (2003) have shown that test dissolution of living *Ammonia becarri* starts at pH 7.0 after five days and can recalcify in standard conditions after eight days. Charrieau et al. (2018c) have shown that *Elphidium crispum* decalcified earlier than *Ammonia* sp. under seawater acidification (respectively nine and 30 days at pH~7.25). These authors also showed that test dissolution occurred even more prematurely in brackish waters (before nine days at pH≤7.53).

Sediment acidification may be link to cable bacteria activity. Cable bacteria (CB) were discovered by Pfeffer and co-workers in 2012. They are sulphide-oxidizing filamentous multicellular procaryotes from the Desulfobulbaceae family. They live in marine and freshwater sediments all around the world (Risgaard-Petersen et al., 2015; Burdorf et al., 2017). They inhabit a several centimetres thick zone from the oxic surface to the deep sulphidic sediment. CB generate a vertical bioelectrical current by coupling the cathodic oxygen or nitrate reduction at the sediment surface to the anodic sulphide oxidation at depth (Nielsen et al., 2010; Pfeffer

et al., 2012; Risgaard-Petersen et al., 2012; Marzocchi et al., 2014). CB activity (CBA) strongly affects sediment geochemistry and results in a clear geochemical fingerprint: an oxygen decrease in the surface sediments combined with a pH maximum in this oxic zone, followed by a strong acidification of the pore water in the suboxic zone (Nielsen et al., 2010; Risgaard-Petersen et al., 2012, 2014; Meysman et al., 2015). It leads to iron sulphide and carbonate dissolution from the suboxic zone (Risgaard-Petersen et al., 2012; Rao et al., 2016; van de Velde et al., 2016) and possibly the calcareous shell of benthic organisms.

Benthic foraminifera live mainly in the topmost sediment. cable bacteria develop also on the few topmost centimetres of the sediment, which can therefore lead to an environmental overlap of the bacterial and foraminiferal communities. Richirt et al 2022 hypothesised that CBA could induce the dissolution of calcareous tests within the sediment of the Lake Grevelingen (Netherlands). In the present study, we assess the impact of cable bacteria activity on the foraminiferal test preservation in sediment, testing the hypothesis that cable bacteria activity is responsible for depleting the preservation of calcareous foraminifera in benthic assemblages. To achieve this, CBA was characterized by oxygen and pH microprofiling and CB density quantified by qPCR on intertidal mudflats of the Auray estuary (French Atlantic coast). Foraminiferal calcareous test dissolution stages were defined and quantified thanks to the analyse of SEM images. Then, we described living and dead foraminiferal assemblages to assess the calcareous test loss.

2 MATERIALS AND METHODS

2.1 Studied Area

The Gulf of Morbihan (Atlantic coast, France) is an enclosed marine bay where the Auray river flows. The Auray estuary is a macrotidal estuary with a tide range about 4 m (**Figure 1**).

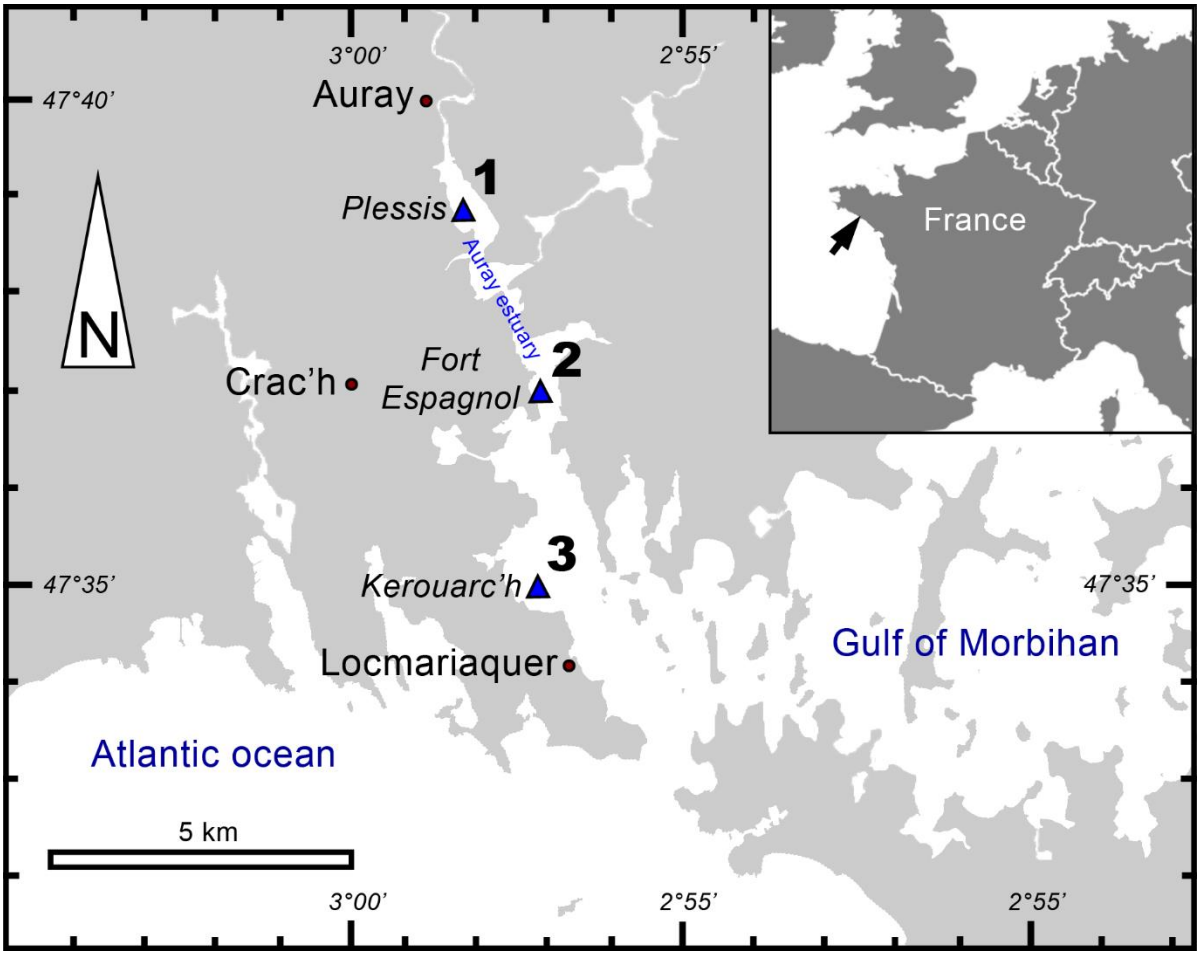

Figure 1. Locations of sampling stations in the intertidal mudflats of the Auray estuary (France).

Saltwater flows upstream over 20 km from the mouth of the estuary (357 m wide) which is tide-dominated (online data from OFB and IFREMER, accessed on May 05th 2022). The extensive description of this area (e.g. the marine influence, hydrodynamics and granulometry) has been reported by Fouet et al. (2022).

In September 2020, three stations along the Auray estuary were sampled on intertidal mudflats at low tide (**Figure 1** and **Table 1**): station 1 (Plessis), station 2 (Fort Espagnol) and stations 3 (Kerouarc'h). Characteristics of the sampled stations are presented in **Table 1**.

Table 1. Characteristics of the stations sampled in September 2020. *Temperature and salinity values correspond to these measured on the sampling day; weighted average and SD of sediment density data from a previous campaign in 2019; (*) name of the station after Fouet et al., (2022).*

Station	Coordinates	Distance from Sea	T (°C)	Salinity	Sediment Density ($g.cm^{-3}$)	Vegetation Cover
1 (*6B)	47.646° N, -2.972° W	12 km	24.4	29.6	1.71 ± 0.12	*Ulvea* mat
2 (*4B)	47.616° N, -2.953° W	8 km	21.2	38.5	1.67 ± 0.33	*Ulvea* mat
3 (*2C)	47.583° N, -2.955° W	4.3 km	21.5	34.3	1.51 ± 0.23	thick *Ulvea* mat few *Zostera*

2.2 Sediment Sampling and Processing

One core was sampled from each station by hand with a Plexiglas® tube (82 mm inner diameter, 50 mm depth) and was transported within an hour in a cool box to the field laboratory. Then, the cores were submerged in ambient seawater for at least two hours to retrieve *in situ* conditions before microprofiling.

After microprofiling, each core was sliced using a core pusher and two trowels. Slice thickness was 2 mm for the first 20 mm depth, and 10 mm up to 50 mm depth. Each sediment slice was treated with Cell-Tracker™ Green (CTG 5 CMFDA: 5-chloromethylfluorescein diacetate; Molecular Probes, Invitrogen Detection Technologies) to mark living benthic foraminifera by fluorescence (Bernhard and Bowser, 1996; Bernhard et al., 2006). One mg of CTG was dissolved in 1 mL of dimethylsulfoxide (DMSO). This solution was then pipetted into the flask containing the sediment slice and its volume of ambient water to get a final solution of CTG about 1 µM (Bernhard et al., 2006; Pucci et al., 2009; Langlet et al., 2013, 2014; Cesbron et al., 2016). Each sample was then incubated in dark at room temperature overnight and then fixed with ethanol 99% (Choquel et al., 2021). Eventually, the samples were quickly and gently sieved with tap water over 315-, 150-, 125- and 63-µm mesh screens. Samples were conserved in 99% ethanol.

DNA was extracted from sub-samples of sediment slices at stations 1 and 2. 1-2 g every second slice down to 18-mm depth were sampled with a heat-sterilized spatula and transferred to 2 ml Eppendorf tubes, then frozen at -20°C degrees. Samples were sent in dry ice ($CO_{2(s)}$ at -50°C) to the Microbiology Institute of Biology in Aarhus University (Denmark) for qPCR analysis to quantify cable bacteria biomass.

2.3 Microsensor Profiling

Two Unisense© profiling systems were used simultaneously. One consisted of two oxygen Clark-type microsensors with a 50-µm diameter tip (Revsbech and Jørgensen, 1986;

Revsbech, 1989), and the other of a pH sensor with a 500 µm tip diameter (PH500, Unisense). They were both mounted on a motorized micromanipulator linked to a computer, and connected to a MultiMeter S/N. The increment was 50 µm until 3 mm for oxygen. It was 100 µm around the seawater-sediment interface (SWI) for pH, and it was adapted in real time according to the evolution of the observed profile until 50 mm depth. For each core, eight descents were managed for O_2, for a total of 16 profiles, while one profiling was done for pH. To calibrate the O_2 microsensor, two points were measured, with the 100% of oxygen saturation in the bubbling seawater column, and the 0% into the anoxic part of sediment. To calibrate the pH microsensor, 3 NBS buffers were used (values 4.0, 7.0, 9.2).

2.4 Living Foraminiferal Analyses

Counts of hard-shell benthic foraminifera were performed in wet conditions (water) on the >125 µm fractions using an epifluorescence stereomicroscope (Olympus SZX12 with a light source CoolLED *p*E-100, emission wavelength λ = 470 nm). All specimens showing clear green fluorescence were picked and identified. Remaining specimens were considered as dead. In doubtful cases, particularly with agglutinated species, specimens were crushed to inspect whether fluorescence was due to the presence of protoplasm, to the autofluorescence of sediment grains composing the test, or the presence of bacteria or nematodes living inside (Langlet et al., 2013; Cesbron et al., 2016). Total foraminiferal densities were expressed per 50 cm^2 of sediment and foraminiferal densities for sediment layers per 10 cm^3 volume.

For the taxonomy of hard-shell foraminifera species, reference publications on estuarine foraminifera (Feyling-Hanssen et al, 1972; Hansen et al, 1976; Murray et al, 1979; Scott et al, 1980; Hayward et al, 2004; Schweizer et al, 2011; Camacho et al, 2015; Richirt et al, 2019; Fouet et al., 2022; Jorissen et al., 2023), and the World Register of Marine Species were used. The distinction between the *Ammonia* phylotypes (Richirt et al, 2019) being difficult, on particular on the dissolved tests, the results will be discussed at the genus level.

2.5 SEM Imaging

Living foraminifera from three layers (0-2 / 6-8 / 40-50 mm depth), according to main pH features, were all observed under a Scanning Electronic Microscope (SEM). Two different high-resolution SEM were used: a DEBEN Hitachi TM4000 at the LPG (samples not metallised, 15kV, wd = 6,5 mm, partial vacuum (60 Pa)) and a Zeiss EVO LS10 at the Service Commun d'Imageries et d'Analyses Microscopiques of Angers University (SCIAM; samples not metallised, 20 kV, wd = 6,5 mm, partial vacuum (60 Pa), amperage 200 to 250 pA). Few scales of calcareous test dissolution of living foraminifera have been proposed in the literature (Corliss and Honjo, 1981; Le Cadre, 2003b; Haynert et al., 2011; Gonzales et al., 2017; Charrieau et al., 2018c, 2022; Schönfeld and Mendes, 2022). These authors proposed scales

varying from 4 to 5 different stages based on SEM images or stereomicroscope observations. They used a wide variety of morphological criteria to describe each dissolution stage (i.e. the number of calcite layers altered and chambers damaged, the presence of cracks or holes, whether the inner organic lining was visible, etc.). In the present study, we propose a scale of six dissolution stages based on SEM pictures of the two most abundant calcareous species in our living assemblages (*Ammonia* spp. and *Haynesina germanica*).

Table 2. Description of the six dissolution stages of the calcareous tests of Ammonia spp. and Haynesina germanica.

DISSOLUTION STAGE	NAME	SEM OBSERVATIONS AND STAGE DESCRIPTIONS	FIGURES
DS-0	Intact test	intact, glassy test with a smooth surface and cylindrical pores, no sign of dissolution.	**Fig. 3-1** **Fig. 4-1**
DS-1	Slight surface dissolved test	transparent test with cylindrical pores, alteration of the last calcite layer only, appearance of the interpore sutures in *H. germanica* (scarce in *Ammonia* spp., alteration more visible on the inter-chamber walls).	**Fig. 3-2** **Fig. 4-2**
DS-2	Peeled test	dull, whitish test with some fusion of adjacent widen pores, calcite layers cracking and crumbling, last chamber often lost, thinner and blunt tubercular ornamentation of *H. germanica.*	**Fig. 3-3** **Fig. 4-3**
DS-3	Cracked test	opaque and cracked test with a strong alteration of all calcite layers, brittle test with holes, fusion of widen pores, the organic lining can be visible, loos of last chamber, broken ornamentation of *H. germanica.*	**Fig. 3-4** **Fig. 4-4**
DS-4	"Star-shape" test	nearly completely dissolved test, only the inter-chamber walls remaining, the last chambers often absent, dissolved peripheral chambers with the inner organic lining visible.	**Fig. 3-5** **Fig. 4-5**
DS-5	Fully dissolved test	totally dissolved test revealing the inner organic lining, may keep the foraminifera shape allowing the identification of the genus *Ammonia* (not observed for *H. germanica*).	**Fig. 3-6**

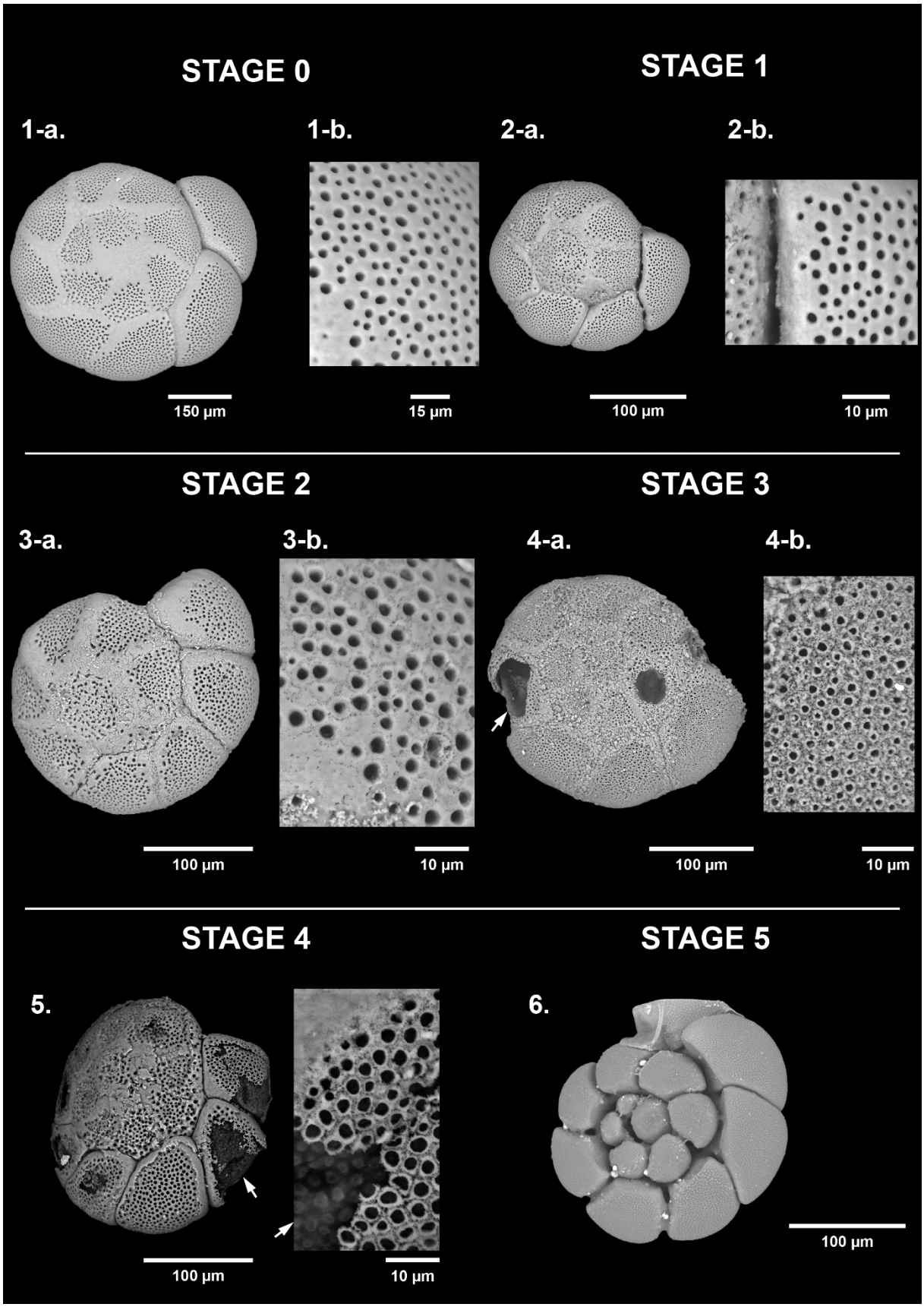

Figure 2. Dissolution scale of Ammonia spp. based on high-resolution SEM images (spiral view). *The specimens are classified into six stages of test dissolution from intact (stage 0) to fully dissolved (stage 5). For stages 0 to 2, a zoom on the last formed chamber was done* ***(1-b, 2-b, 3-b)****, and on the n-1 chamber for stage 3* ***(4-b)****. White arrows point the organic lining.*

173

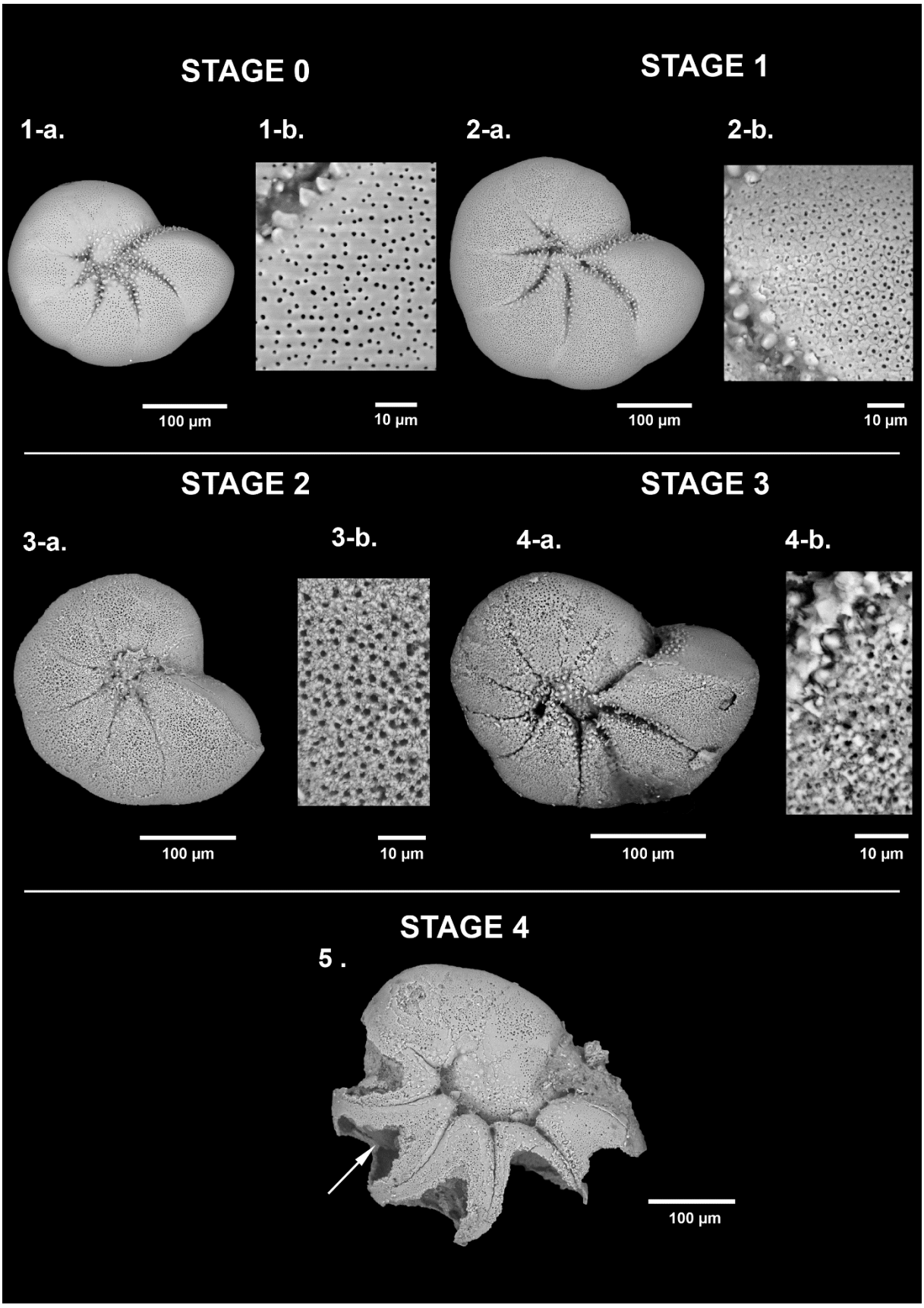

Figure 3. Dissolution scale of Haynesina germanica based on high-resolution SEM images. *The specimens are classified into five stages of test dissolution from intact (stage 0) to the « star shape » (stage 4). No organic lining (stage 5) has been identified as belonging to the taxa Haynesina. For stages 0 and 1, a zoom on the last formed chamber was done (**1-b, 2-b**), and on the n-1 chamber for stages 2 and 3 (**3-b, 4-b**). White arrow points the organic lining.*

174

2.6 Dead Foraminiferal Analyses

Non fluorescent tests of foraminifera were counted as dead specimens and picked in wet conditions (water) to preserve the organic linings from fully dissolved tests. We proceeded under a stereomicroscope (ZEISS Stemi sv11) in three sediment layers: the surface layer (0-2 mm), the subsurface layer (6-8 mm) and the deep layer (40-50 mm). After quick observations, when high densities were estimated (above 500 individuals; Patterson and Fishbein, (1989)) fractions were splitted into 8 sub-samples using a wet splitter (Charrieau et al., 2018a).

2.7 Ratios in Foraminiferal Assemblages

In order to characterize the loss of calcareous specimens in the assemblages, we defined a ratio enabling each sample to be compared as follows:

$$C/T = calcareous\ foraminifera/total\ foraminifera$$

Calcareous foraminifera are counted regardless their dissolution stage and total foraminifera include agglutinated individuals. To estimate the intensity of dissolution in the assemblage, we calculated the following ratio:

$$DS\text{-}5/C = calcareous\ test\ at\ dissolution\ stage\ 5/total\ calcareous\ foraminifera$$

These ratios were calculated on both living and dead assemblages for layers 0-2 / 6-8 and 40-50 mm.

2.8 Statistical Procedure

The putative relationship between cable bacteria activity and the advanced dissolution stages of the living calcareous test foraminifera was assessed by applying the parametric Fisher's test followed by the pair-wise Fisher's test for *post-hoc* comparisons were used. To minimize the risk type 1 error *p*-values were FDR-adjusted. The significance level was set to 5 %. As the last layer of calcite produced during the growth of the foraminifera covers the entire test and is thinner than the others (Haynes, 1981; Hansen, 1999; Debenay et al., 2000; Boudagher-Fadel, 2018), DS-1 and 2 are more commonly observed resulting from a process of gradual dissolution or precipitation of calcite. Discrimination of the effect of the dissolution process is therefore made on the alteration of several calcite layers as for DS-3 and above. For this purpose, the dissolution stages were combined into two groups: no to slight dissolution (DS-0, 1 and 2) and moderate to severe dissolution (DS-3, 4 and 5). These two groups were then compared between each of the three stations, and between the different depth levels (0-2 / 6-8 / 40-50 mm depth) for each station. Statistics were carried out using the *R* software using the "stats" and "rstatix" packages.

2.9 Sediment Treatment for DNA Extraction and Quantification

DNA was extracted from weighed amounts of sediment (0.22 - 0.25 g wet weight). DNA extraction was carried out using DNeasy PowerLyzer PowerSoil Kit (Qiagen) and the DNA was collected in 60 µl elution buffer. The analysis followed the procedures outlined in Geelhoed et al. (2020). The primer combination of ELF645wF and CB836wR was used to target the 16S rRNA gene of the marine cable bacteria of the genus *Candidatus* Electrothrix Trojan, 2016. The calibration curves were obtained using a synthetic standard (sequence accession KR912339.1, position 611-912, synthesized by Eurofins Genomics, Denmark) diluted in a 10-fold dilution series. The standards and samples were run in triplicates. Each reaction contained the master mix (RealQ Plus 2x Master Mix Green, Low ROXTM, Ampliqon, Denmark), forward and reverse primers (0.2 µM), BSA (1 µM). The qPCR was performed with a real time PCR analyser (AriaMX, Agilent). The thermal cycles were as follows: 15 min at 95 °C for initial denaturation followed by 40 cycles of 15 s at 95 °C (denaturation), 30 s at 60 °C (annealing), and 20 s at 72 °C (amplification). Afterwards, the melting curve was obtained by 30 s at 95°C, 30 s at 60 °C, and 30 s at 95 °C. Finally, the temperature was held for 5 min at 40 °C to terminate the analysis. The results are reported as the unit gene copies.(g wet sediment) $^{-1}$. CB filament density were calculated as in Geelhoed et al. (2020), using data of wet sediment density from a previous campaign in 2019 (**Table 1**), and expressed in m.cm^{-3}. For administrative reasons, it was only possible to carry out these DNA analyses for stations 1 and 2.

3 RESULTS

3.1 Microsensor Profiles and Cable Bacteria Abundance

Oxygen penetration depth in the sediment at stations 1, 2 and 3 was 1.4 ± 0.2, 0.9 ± 0.3 and 0.9 ± 0.2 mm, respectively. At station 1, pH rapidly decreased from 7.7 at the Sea Water Interface (SWI) to a minimum of 6.8 at 15 mm depth. Below this minimum, pH stabilised to 7.2 around 40 mm depth. In contrast, at stations 2 and 3, pH increased immediately below the SWI from 7.8 to 8.1 at 0.8 mm depth and to 7.95 at 0.6 mm, respectively (**Figure 4**). Below these maxima, at both stations, pH reached a minimum of 5.8 at 7 mm depth at station 2 and of 6.3 between 7-19 mm depth at station 3. Below these minima, pH stabilised at 6.8 after 25 mm depth at station 2, and at 6.9 after 34 mm depth at station 3.

At station 1, the number of 16S CB copies of *Candidatus* Electrothrix ranged from 0.23 ± 0.01 $_x10^7$ to 0.48 ± 0.01 $_x10^7$ 16S copies.(g wet sediment)$^{-1}$, and remained constant through depth (**Figure 4**). At station 2, it amounted to 2.8 ± 0.12 $_x10^7$ 16S copies.(g wet sediment)$^{-1}$ in the upper 5 mm of sediment and progressively decreased to about 0.3 ± 0.01 $_x10^7$ 16S

copies.(g wet sediment)$^{-1}$ in the 16-18 mm depth layer. The maximum 16S CB copies of *Ca.* Electrothrix in station 2 corresponded to the maximum pH in depth. According to Geelhoed et al. (2020) and using wet sediment density from the same stations obtained in 2019 (pers. comm. M. Fouet), we calculated a filament density of 7.4 ± 0.4 and 74.4 ± 5.0 m.cm^{-3} at stations 1 and 2 respectively.

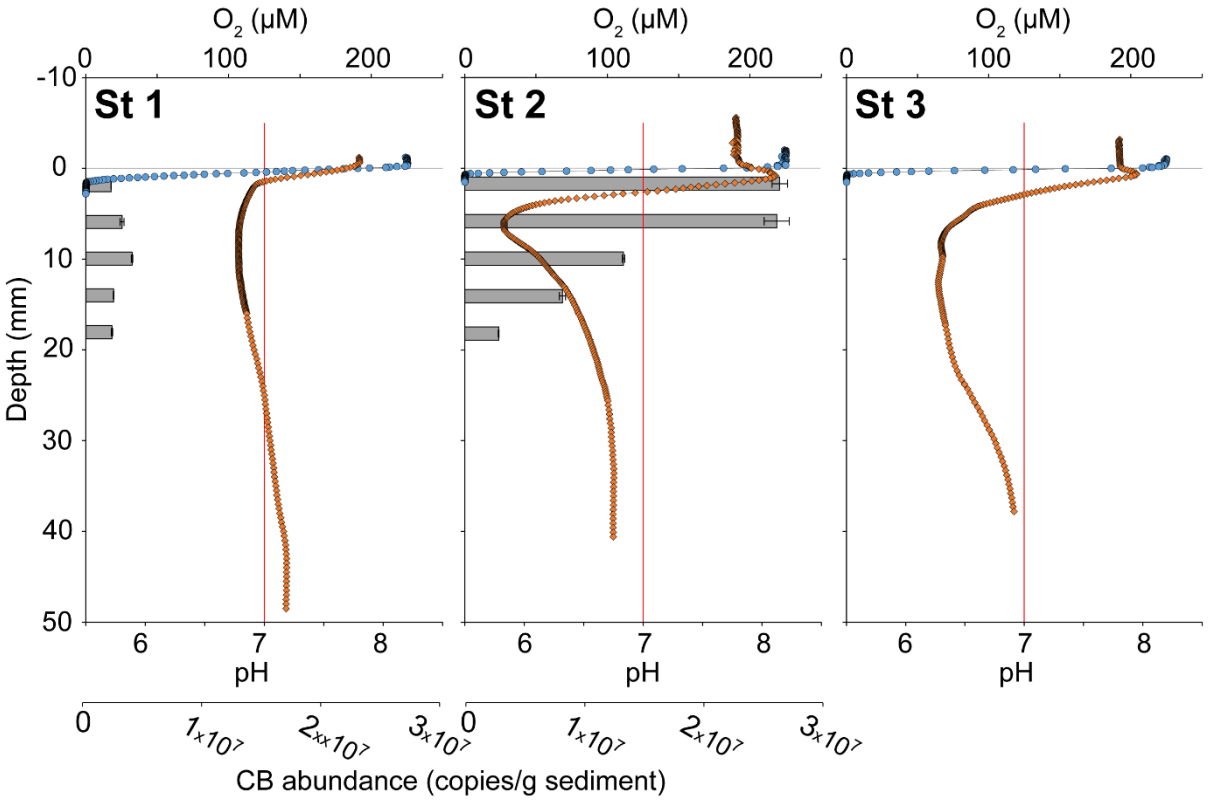

Figure 4. Sediment oxygen (blue circles) and pH (orange diamonds) microprofiles at the three stations, and vertical distribution of cable bacteria abundance (qPCR of Ca. Electrothrix 16S rRNA gene copies, grey bars) for stations 1 and 2. *0 is the position of the Sea Water Interface (SWI). The vertical red line represents neutral pH. The oxygen profile presented is one of those obtained by microprofiling, and representative of O_2 penetration for each station.*

3.2 Hard-Shelled Benthic Foraminiferal

3.2.1 Living Foraminiferal Diversities and Densities

The foraminiferal species assemblages were typical of the estuarine environments (Debenay et al., 2000), with a poor species richness (14, 13 and 18 species at stations 1, 2 and 3 respectively). *Ammonia* spp. and *Haynesina germanica* (Ehrenberg, 1840) both strongly dominated the assemblages at all three stations (25.1 and 51.5 % respectively of the total assemblage for station 1, 14.5 and 48.2 % for station 2, 7.3 and 61.4% for station 3; **Figure 5**). *Ammonia* spp. included the species *Ammonia veneta* (Schultze, 1854) (phylotype T1 after Hayward et al., 2004), *Ammonia aberdoveyensis* Haynes, 1973 (phylotype T2 after Hayward et al., 2004), and *Ammonia confertitesta* Zheng, 1978 (phylotype T6 after Hayward et al., 2004). Agglutinated foraminifera represent 19.9, 25.7 and 12.7 % of the total assemblage at

stations 1, 2 and 3, respectively. They were dominated by *Ammobaculites agglutinans* (d'Orbigny, 1846).

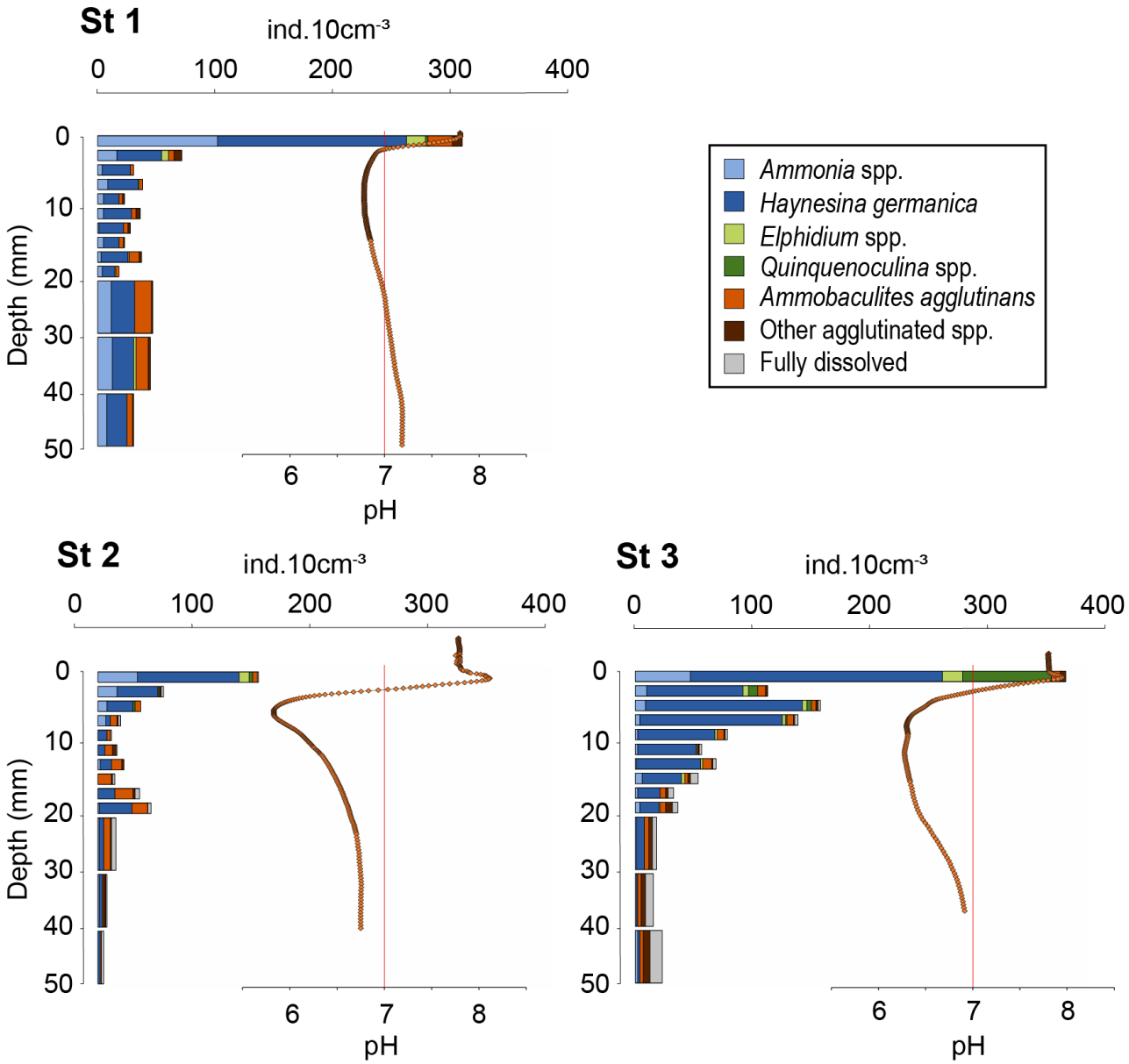

Figure 5. Vertical distributions of living-foraminifera densities per 10 cm³ of sediment at the three stations (>125 µm fraction). *0 is the position of the Sea Water Interface (SWI). Recall of pH microprofiles (orange diamonds) and neutral pH (vertical red line).*

3.2.2 Living Foraminiferal Vertical Distribution

Total densities of CTG-labelled foraminifera in cores 1, 2 and 3 were 1273, 548, and 1431 ind.50cm^{-2} respectively. Highest densities were found in the first layer of sediment (0-2 mm depth) for all cores with 295, 137 and 371 ind.10cm^{-3} at stations 1, 2 and 3, respectively (**Figure 5**), where dioxygen was available and pH was maximal (**Figure 4**).

At station 1, total density dropped below 2 mm to stabilize at 30 ± 9 ind.10cm^{-3} (**Figure 5**). At station 2, the vertical distribution of total densities showed two maxima. The first at the SWI and a second at 18-20 mm depth with 47 ind.10cm^{-3}. A first minimum of 11 ind.10cm^{-3}

was observed at 8-10mm depth close to the lowest pH layer and a second minimum of 5 ind.10cm^{-3} was observed at the bottom of the core. At station 3, after a maximum at the SWI, foraminifera density decreased gradually with depth, following the pH trend, to reach on average 19 ± 4 ind.10cm^{-3} from 20 to 50 mm depth.

At station 1, the ratio of calcareous foraminifera in the living foraminiferal assemblage (C/T) was 0.91 for the SWI (**Table 3**) and around 0.77 ± 0.07 for the layers below. At station 2, C/T was 0.97 of the SWI and on average 0.64 ± 0.16 between 2 and 50-mm depth (**Appendix**). However, agglutinated taxa dominated the assemblages from 10 to 18 mm, just below the pH minimum, with a drop of C/T ratio to 0.39 ± 0.18 (**Appendix**). At station 3, the C/T ratio was 0.97 at the SWI and decreased asymptotically as calcareous foraminiferal densities vanished to reach 0.72 ± 0.15 below 20 mm after the pH minimum zone (**Appendix**).

3.2.3 Calcareous Test Dissolution of Living Foraminifera

Figure 6 shows the dissolution stage (DS) of calcareous foraminifera for three selected sediment layers (0-2 / 6-8 / 40-50 mm) for living assemblages. At station 1, living specimens with calcareous test showed low alteration. The DS remained stable through depth ($p > 0.05$). Specimens with “Intact tests” (DS-0) or “slight surface dissolved tests” (DS-1) represented 90 % of calcareous foraminifera. The strongest dissolution stages were DS-2 (“peeled test”) and DS-3 (“cracked test”) accounting for less than 10 %.

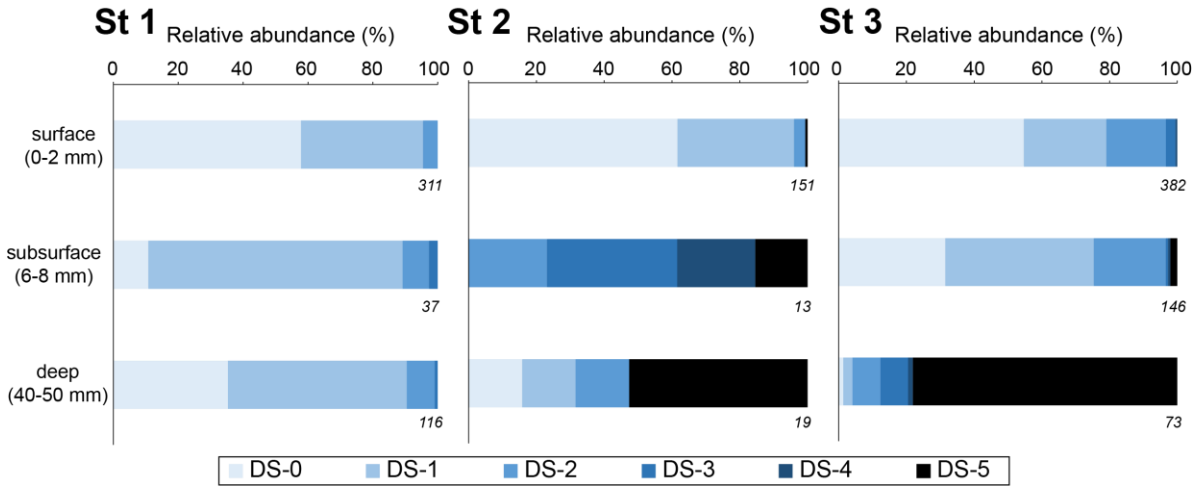

Figure 6. Relative abundance of living benthic foraminifera with calcareous test for each dissolution stage for 10 cm^3 of sediment (Ammonia spp. and H. germanica from the >125 µm fraction). *Three depth levels were analysed: the surface (0-2 mm; oxic zone), the subsurface (6-8 mm; suboxic zone corresponding to pH minimum), and the deeper (40-50 mm; anoxic zone). The numbers on the lower right of the boxes are the total numbers of SEM photographed specimens.*

Conversely, at station 2, many foraminifera were very fragile under manipulation. Numerous “fully dissolved tests” (DS 5) with only the organic lining were observed through depth (50 ind.50cm^{-2}; **Appendix**). At the SWI (0-2 mm layer), DS-0 and DS-1 tests represented 95% of the calcareous test foraminifera in the living assemblage. Only few DS-2 and DS-5 specimens were present. In the subsurface level (6-8-mm depth), corresponding to the most

acidic conditions, no DS-0 and DS-1 specimen was observed. DS-4 and DS-5 tests were about 40 % of the calcareous tests observed. At the deepest layer (40-50 mm), DS-5 specimens were dominant (>50 %). The surface layer was significantly different ($p < 0.005$) from the two deeper layers that showed no significant differences ($p = 0.267$).

At station 3, many foraminifera were fragile under manipulation, and DS-5 specimens were abundant through depth with about 140 ind.50cm^{-2} (**Appendix**). At the SWI (0-2 mm layer) and in the subsurface level (6-8-mm depth), DS-0 and DS-1 specimens represented about 75 % while DS-2 accounted for 20 %. Few specimens of DS-3, DS-4 and DS-5 were observed. At the deepest layer (40-50 mm), DS-5 specimens were the most abundant calcareous tests foraminifera (78 %). The severe DS (DS-3, 4 and 5) were significantly overrepresented in the deep layer than in the surface and subsurface layers ($p < 0.005$). DS were not significantly different between surface and subsurface ($p = 1$).

Overall, the exact Fisher's test revealed significant difference dissolution stages among stations ($p<0.005$). The pair-wise Fisher's exact test showed that the low DS (0,1,2) were significantly overrepresented at station 1 compared to the two other stations ($p<0.005$). Furthermore, there were no significant difference between stations 2 and 3 ($p=0.532$).

3.2.4 Calcareous vs. Agglutinated Foraminifera in the Dead Assemblages

Species in the benthic foraminiferal thanatocoenosis were the same as in the living assemblages. At station 1, calcareous taxa dominated agglutinated ones in the dead assemblage with C/T ratio varying from 0.74 to 0.89 (**Table 3**). The proportion of organic lining (DS-5/C) increased slightly with depth, from 0.06 to 0.18. On the other hand, at station 2, agglutinated taxa dominated the dead assemblage in the surface and subsurface levels (C/T ratio of 0.43 and 0.36 respectively) but not in the deepest one even if they remained abundant (0.65; **Table 3**). The DS-5/C ratio was very high in all three depth layers, remaining >0.70. At station 3, C/T ratio remained high in the dead assemblage of both surface and subsurface with 0.88, 0.83, and decreased strongly to 0.36 in depth where agglutinated specimens were dominant. The DS-5/C ratio increased with depth, from 0.06 at the surface to 0.95 in the deeper layer.

Comparing dead and living assemblages, it can be noted that for station 1, C/T ratio were not very different whatever the depth (**Table 3**). Stations 2 and 3 showed much lower C/T ratios in the dead assemblages indicating a marked loss of calcareous foraminifera during taphonomic processes although this difference is not significant. In addition, stations 2 and 3 showed a higher occurrence of DS-5 tests in the dead assemblages resulting in high DS-5/C ratios. In detail, station 2 showed the highest DS-5/C ratio in the subsurface layer (0.96) where pH is minimal, while station 3 showed a strong increase of this ratio in the deepest layer (0.95).

Table 3. Densities of living and dead foraminifera for each depth layer at the three all stations (ind.10 cm^{-3} of sediment). *Depth correspondences: surface (0-2 mm), subsurface (6-8 mm) and deep (4-5 mm). "Calcareous" class includes the DS-5 specimens (fully dissolved test showing the organic lining). A = agglutinated, C = calcareous, ratios are those described in the methods.*

		Living foraminifera					Dead foraminifera				
		Agglutinated (A)	Calcareous (C)	Fully dissolved test (DS-5)	C/T ratio	DS-5/C ratio	Agglutinated (A)	Calcareous (C)	Fully dissolved test (DS-5)	C/T ratio	DS-5/C ratio
St 1	surface [0-2 mm]	30	295	0	0.91	0.00	212	589	38	0.74	0.06
	subsurface [6-8 mm]	3	36	0	0.92	0.00	21	153	22	0.88	0.14
	deep [40-50 mm]	6	26	0	0.81	0.00	94	772	141	0.89	0.18
St 2	surface [0-2 mm]	4	137	1	0.97	0.01	373	282	197	0.43	0.70
	subsurface [6-8 mm]	7	12	2	0.63	0.17	181	104	100	0.36	0.96
	deep [40-50 mm]	1	4	2	0.80	0.50	239	453	327	0.65	0.72
St 3	surface [0-2 mm]	12	371	0	0.97	0.00	58	418	49	0.88	0.12
	subsurface [6-8 mm]	7	137	3	0.95	0.02	45	214	53	0.83	0.25
	deep [40-50 mm]	9	14	11	0.61	0.79	493	274	259	0.36	0.95

4 DISCUSSION

4.1 Is Cable Bacteria Activity Responsible for Porewater Acidification in the Mudflats of the Auray Estuary?

Oxygen and pH microprofiles recorded at stations 2 and 3 showed the typical fingerprint of cable bacteria activity (CBA): a pH maximum within the oxic zone without oxygen production followed by a significant acidification into the suboxic zone (**Figure 4**; Nielsen et al., 2010; Pfeffer et al., 2012; Risgaard-Petersen et al., 2012; Meysman et al., 2015). The presence of cable bacteria within the upper first centimetre at station 2 was further confirmed by the qPCR data. The calculated filament density of about 70 m.cm^{-3} at this station was in the same order of magnitude than the *in situ* densities reported from the Baltic sea (Marzocchi et al., 2018; Hermans et al., 2019), from bivalve reefs (Malkin et al., 2017), subtidal mudflats (van de Velde et al., 2016) or intertidal salt marshes (Larsen et al., 2015). The geochemical signature at station 1 is less clear regarding CBA although the qPCR data indicated CB filament density in the low range of the *in situ* densities reported from the Baltic sea (Marzocchi et al., 2018; Hermans et al., 2019).. Here, there was no pH peak in the oxic zone and the suboxic acidification was the weakest compared to stations 2 and 3 (ΔpH < 1.0 and ΔpH of 2.3 and 1.6 respectively). As the sediment acidification continued at least 5 mm below the oxic zone (oxygen penetration depth < 2-mm depth) for the three stations, oxic processes such as pyrite oxidation are unlikely to explain such pH decrease. However, the anaerobic oxidation of reduced compounds such as manganese, iron or sulphide, could be involved in the porewater

acidification (Soetaert et al., 2007; Middelburg et al., 2020) but the observed acidification was too high to be explained by such processes (van Cappellen and Wang, 1996; Soetaert et al., 2007). Therefore, we suggested that acidification was mainly driven by cable bacteria activity rather than any other geochemical process.

The diversity of pH microprofiles observed between the three stations could indicate a contrasted intensity of the cable bacteria activity between stations. According to the low filament abundance and the low range of pH (ΔpH = 1.0) at station 1, CBA would be minimal and it would have limited impact on the sediment geochemistry. Conversely, the strong abundance and pH range (ΔpH = 2.4) suggest the most intense cable bacteria activity at station 2, whereas pH range (ΔpH = 1.8) at station 3 suggests an intermediate to high CBA. It is possible that such variability from a mudflat to another can be explained by the stage of development of the bacterial community and/or by the specific geochemical composition of each mudflat from upstream to downstream (Malkin et al., 2014, 2017; Rao et al., 2016). Our observations suggest that *Ulvae* mats observed at stations 2 and 3 during core sampling in autumn (**Table 1**) could play a role on CB development. Several studies showed that macrophyte decay is rather slow compared to microphytobenthic mineralization and favours free-sulphide production and upward diffusion (Anschutz et al., 2007; Metzger et al., 2007; Cesbron et al., 2014; Delgard et al., 2016) which are favourable conditions to CB development. Previous observations confirm the spatial and seasonal cable bacteria activity dynamics (e.g. Seitaj et al., 2015; Lipsewers et al., 2017; Hermans et al., 2019; Malkin et al., 2022). Most publications refer to a boom-and-bust cycle of CB in laboratory incubations, and to the seasonal alternation of the sulphur-oxidising bacterial community in the field as a function of hypoxia events inducing seasonal pH variability. However, no desoxygenation or strong and recursive reworking events have been reported in the present studied area during the previous weeks before sampling, which is reoxygenated at each low tide (Fouet, 2022; OFB and IFREMER data). Each low tide could lead to the reactivation of cable bacteria activity in these highly eutrophic mudflats. The most intense resuspension phenomenon here would be rising tide (Menier and Dubois, 2011; Menier et al., 2011) and bioturbation. The benthic macrofauna (> 2 mm) of the mudflats is dominated by polychaetes *Nephtys* spp. known to burrow into the sediments (Michaud et al., 2021; abundance around 8 ind.50cm^{-2}, pers. comm. Oihana Latchere). The variability between the stations could be the result of bioturbation modulating acidification within subsurface sediment layer (Malkin et al., 2014, 2017, 2022; Aller et al., 2019). Unfortunately, there is little literature on cable bacteria activity under tidal cycle. Currently, the control factors of spatial and temporal discrepancies of the cable bacteria density and the CBA are still unresolved and need more investigations.

The cable bacteria activity causes pH anomalies that impact sediment geochemistry and lead to the carbonate dissolution process as described in Risgaard-Petersen et al. (2012), Meysman et al. (2015), Rao et al. (2016), van de Velde et al. (2016) and Malkin et al. (2017). It has been supposed that this dissolution process could be responsible for foraminiferal test dissolution (Risgaard-Petersen et al., 2012; Richirt et al., 2022). Considering the increase of observations of cable bacteria activity occurrence in a wide range of coastal and marine environments (Burdorf et al., 2017; Scholz et al., 2021), we assume that the potential impact of this bacterial acidification of sediment on carbonate meiofauna should be strongly considered.

4.2 Impacts of Sediment Acidification on Living Foraminifera

We showed in **Figure 4** and **Figure 6** that advanced dissolution stages 3, 4 and 5 were significantly overrepresented at stations 2 and 3, where acidification was important, compared to station 1 where no DS-5 was observed. More precisely, vertical DS distribution corresponded to vertical acidity variability at stations 2 ($0.01 < DS\text{-}5/C < 0.50$) and 3 ($0.00 < DS\text{-}5/C < 0.79$). There was no indication for such depth distribution at station 1 where pH variability was the lowest ($DS\text{-}5/C = 0$). The relative abundance of calcareous specimens over agglutinated (C/T) was very stable along depth at station 1 (0.78 ± 0.07; **Appendix**) whereas this ratio was more variable at stations 2 and 3 (0.65 ± 0.17 and 0.73 ± 0.15 respectively), confirming that pH conditions affected the assemblage composition through the under representation of calcareous foraminifera (**Figure 5**) . Species diversity appeared to not be affected because most of the foraminiferal population lived in the thin oxic zone, which is not affected by the strong pH decrease. Our data suggest that the sediment acidification on the mudflats, supposedly due to cable bacteria activity, has a drastic effect on the integrity of living benthic foraminiferal test and potentially on their assemblages. The magnitude of this effect may depend in the dissolution process intensity and duration throughout the life cycle of foraminifera.

Since the dataset of the present study is rather limited, one can examine literature data that provides together oxygen and pH microprofiles with sub-centimetre vertical distribution of living foraminifera in intertidal mudflats first and other benthic environments. Geochemical data from an intertidal mudflat of the Arcachon basin in the French Atlantic coast suggest sediment acidification in May 2011 at station N (Cesbron et al., 2016) with a $\Delta pH = 1.6$ and a pH minimum of 6.2 well below the oxic zone at 20-mm depth. At the same station in July 2011, all calcareous benthic foraminifera specimens showed a fully dissolved test with the organic lining remaining ($DS\text{-}5/C = 1$). The assemblage also showed that, *Eggerella scabra*, an agglutinated species, strongly dominated the foraminiferal assemblage at all depths down to 50 mm, except for the 0 to 5 mm layer ($C/T = 0.88 \pm 0.02$ for the uppermost layer; $C/T = 0$ below). The authors

assumed that test dissolution resulted from a strong acidification of the sediments due to an intense remineralisation of the relict roots of *Zostera*. We can assume here that these roots provided the refractory material that enhanced sulphate reduction (Anschutz et al., 2007; Metzger et al., 2007; Cesbron et al., 2014; Delgard et al., 2016), providing enough free-sulphide to favour cable bacteria development that could drive the dissolution process as it probably happened at stations 2 and 3 of the Auray estuary in the present study. However, Cesbron and co-workers also showed that during winter (February 2011), foraminifera showed less dissolution due to a lower intensity of diagenetic processes including free-sulphide production and probably benthic acidification. These results underline the importance of the temporal variability of diagenetic processes that influence pore water geochemistry and eventually calcareous test integrity. It also questions about time integration of pH conditions recorded in the foraminifera tests as foraminifera may have mechanisms to buffer pH variations as suggested by different studies (de Nooijer et al., 2009b, 2014; Toyofuku et al., 2017) or vertical migration strategies (Geslin et al., 2004; Pucci et al., 2009; Koho et al., 2011; Hess et al., 2013). It could be assumed that the dissolution of the calcareous foraminifera tests would respond to integrated dynamics over a few days to a few weeks (Le Cadre, 2003; Charrieau et al., 2018b, 2022; Daviray, pers. com.). These microorganisms are capable of recalcifying their test following acidification events with the same daily to weekly dynamics (Le Cadre et al., 2003). This dynamic is relatively comparable to the oxidation processes of the reduced mineral phases that can generate acidification of the sediment as is cable bacteria activity. We therefore assume that the tests of dead specimens incorporate the variability of these dynamics to a greater or lesser extent. These dynamics should be investigated in the future in Auray estuary to better understand differences of dissolution stages observed between stations. It can also be assumed that tolerance to acidification may be species-dependent. Under laboratory experiments, Charrieau et al. (2018) have shown that *Ammonia* sp. specimens survived longer than *Elphidium crispum* under the same conditions of salinity, pH and Ω_{calc} (20-34, 7.3-7.9 and 0.4-2.7 respectively). Mojtahid et al. (2023) have observed that low DIC (< 900 µmol.kg^{-1}) affected growth and survival of *Bulimina marginata* and *Cassidulina laevigata* but not *Ammonia confestitesta*, while a pH and Ω_{calc} decrease did not affect any of the three species (other parameters constant, pH > 7.5, $\Omega_{calc} \geq 1$). McIntyre-Wressnig et al. (2014)have seen no effect of acidification on *Bolivina argentea* and *Bulimina marginata* (S~34, TA~2400 µmol.kg^{-1}, pH ≥ 7.5). Furtermore, Haynert et al. (2011) have shown that *Ammonia aomoriensis* slightly decalcified as soon as pH~7.7 and $\Omega_{calc} > 1$, and showed severe dissolution at pH ≤ 7.4 and $\Omega_{calc} < 1$. However, the same species cultured in their natural sediment was unaffected in the same geochemical conditions (Haynert et al., 2014). It suggests that sediment chemistry provides a microhabitat to support benthic foraminiferal community growth and development even under sediment acidification. These interesting

457 results have emphasized the complex and misunderstood interaction between calcareous test
458 foraminifera and the carbonate system that need more detailed investigations.

459 Conversely, a tidal mudflat from another estuarine system of French Atlantic coast
460 seems not to show indices of acidification process nor occurrence of dissolution on living
461 foraminifera. Living foraminifera form the Brillantes mudflat of Loire estuary was studied at two
462 stations in September 2012 and April 2013 (Thibault de Chanvalon et al., 2015, 2022). The
463 vertical distribution of living foraminifera reported in the Loire mudflat was similar to the vertical
464 distribution of station 2 reported in the present study with a maximal density at the topmost
465 layer within the oxic zone, a minimal density around 10-mm depth and a second maximum
466 below. However, no foraminiferal test dissolution was reported by Thibault de Chanvalon and
467 co-workers and the foraminiferal assemblages were heavily dominated by calcareous
468 foraminiferal species, resulting in a DS-5/C ratio equal to zero and a C/T ratio about 1.
469 Furthermore, at these stations, pH profiles did not show strong acidification or CBA fingerprint
470 at different occasions (May 2013, February 2014, June 2018, unpublished data). pH decrease
471 corresponded to oxygen uptake and was below 0.5 units with a minimum about 7.7. No pH
472 peak at the interface was observed in a profile performed in the dark neither. The major
473 difference between these systems is the size of the river that induces significant resuspension-
474 deposition events for the Loire estuary (network SYVEL, GIP Loire Estuaire). In addition,
475 bioturbation seems to be intense at the Brillantes mudflat (Thibault de Chanvalon et al., 2015,
476 2016b, 2017). Another difference between these studies is the absence of macrophytes at the
477 studied stations of the Brillantes mudflat. Finally the size of the catchment area of Loire
478 provides an important flux of suspended particles rich in metallic oxides that will once settled
479 in the mudflat generate a thick layer of sediment where the iron cycle dominates diagenetic
480 processes acting as an efficient “iron curtain” that maintains free-sulphide between 5 to 10 cm
481 depth (Thibault de Chanvalon et al., 2016a, b). These combined conditions are not favourable
482 to cable bacteria development (Malkin et al., 2014, 2017). This, foraminiferal observations
483 strongly suggest the absence of dissolution process in the studied part of the Brillantes mudflat.
484 This area may be considered as a control station.

485 Other studies reporting calcareous test dissolution of benthic living foraminifera in
486 transitional environments are published but without geochemical data, allowing to discuss
487 potential causes of the dissolution process(Alve and Nagy, 1986; Buzas-Stephens, 2005;
488 Polovodova and Schonfeld, 2008; Bentov et al., 2009; de Nooijer et al., 2009; Kurtarkar et al.,
489 2011; Haynert et al., 2012; Schönfeld and Mendes, 2022). Although the hypotheses put
490 forward by these authors on the causes of test dissolution are all plausible (environmental
491 pollution, freshwater inputs, organic matter degradation), they are not strongly explained.
492 Therefore, the absence of pH data (Buzas-Stephens, 2005; Polovodova and Schonfeld, 2008)

or its insufficient vertical resolution (Alve and Nagy, 1986; Haynert et al., 2012; Schönfeld and Mendes, 2022) do not exclude the potential involvement of cable bacteria in those environments. In the Baltic sea, that could be considered as a sort of giant estuary, Charrieau et al. (2018a), provide pH microprofiles that seem to indicate the absence of strong acidification (all sites combined: minimum pH = 7.17; maximum ΔpH = 0.6). However, these authors observed calcareous test dissolution of living foraminifera and concluded that dissolution may be the consequence of a complex set of environmental factors whose ecological equilibrium can change rapidly in such coastal areas (salinity, oxygen concentration, pH and Ω_{calc}). Laboratory experiments conducted by these authors (Charrieau et al., 2018b), seem to indicate that low salinity may be an important factor on calcareous test dissolution. The difference with estuarine studies discussed above is probably that salinity change dynamics in the Baltic is rather minor compared to salinity in Auray and Loire that are macrotidal systems with species adapted to such salinity variations.

4.3 Impacts of Sediment Acidification on Dead Assemblages and Shell Preservation

Richirt et al. (2022) have assumed that calcium carbonate undersaturation in suboxic zone resulting from cable bacteria activity could be responsible for low densities of calcareous tests in the dead assemblages recorded in sediments of Lake Grevelingen. Our results suggest that acidification, as CBA could induce, strongly affects the calcareous test integrity and the assemblage composition of living foraminifera before taphonomic processes. Our study also suggests that after foraminifera death, dissolution processes keep transforming the foraminifera assemblage during test burial supporting the hypothesis formulated by Richirt and coworkers (2022). Comparing C/T and DS-5/C ratios between living and dead assemblages at different depths we relate in detail the impact of pH distribution to the taphonomic loss. Under a low acidification (like at station 1), calcareous tests were relatively well preserved. At this station, the community structure between living and dead assemblages varied slightly (C/T ranged from 0.81- to 0.98 in living assemblage and from 0.74- to 0.89 in dead assemblage). The occurrence of dissolution in the living assemblage was nil while in the dead assemblage the DS-5/C ratio increased with depth from 0.06 to 0.18 indicating that the low dissolution generated a relatively slow taphonomic process. Calcareous tests dominated both living and dead assemblages with an increase of this trend with depth in the dead assemblage confirming the good preservation of calcareous foraminifera. Where sediment acidification was moderate (like at station 3), the dissolution effect on the thanatocoenosis was gradual with depth. Calcareous test density decreased through the wide acidic layer (C/T decrease from above 0.8 to 0.36 at 50-mm depth) and there was an accumulation of fully dissolved tests showing only their organic linings in dead foraminiferal assemblages at depth (DS-5/C of 0.95). This

feature suggests that the moderate dissolution generated a gradual taphonomic process leading to a noticeable calcareous loss with depth. Eventually, under a strong and intense dissolution process (like at station 2), the effect occurred mostly within the restricted acidic layer. The calcareous tests disappeared from the dead foraminiferal assemblage in this subsurface layer while the fully dissolved tests showing only their organic linings and agglutinated tests accumulated (C/T = 0.37 and DS-5/C = 0.96). At depth, the dead foraminiferal assemblage showed fairly high densities that are comparable to stations where acidification was less intense. As the living specimens were quite rare, such accumulation of dead tests suggested that somehow they bypassed the acidic firewall of the suboxic layer. If tests arrived at depth through sedimentary burial the acidic firewall was possibly variable through time and not constantly established. If sediment acidification is more constant, physical or biological reworking buried sufficiently fast to preserve tests from corrosive conditions and mechanic crumbling. Here, regardless of the alkalinity or calcium carbonate content of the sediment, if living and dead calcareous foraminifera are decalcified so intensely, the corrosive conditions are intense enough over time to generate dissolution in organisms, which alive can fight off these hostile conditions to a greater or lesser extent, as they are somehow adapted to the strong physical and biogeochemical dynamics of transitional environments.

At this stage, these hypotheses cannot be assessed. One can note the high concentration of dead fully dissolved tests in the first 2 mm (0.70) where pH is the most alkaline suggesting that sedimentary reworking may have brought dead specimens from the subsurface acidic layer to the surface. Further studies on dead assemblages are needed to statistically validate the CBA vs. calcareous test loss relationship.

With low pH and carbonate undersaturation in pore water, the dissolution process resulting from cable bacteria activity could leave an imprint on taphonomy and on historical records yet to be explored. Indeed, it may alter the carbonate composition of the remaining calcareous tests used to geochemical proxies based on isotopic fractioning or trace elements (Katz et al., 2010; Petersen et al., 2018; Mojtahid et al., 2023).

In this case, CBA may be considered as a potential factor in the seasonal perturbation of sediment geochemistry in interpretations of foraminiferal assemblages of historical studies. As proposed in Richirt et al. (2022), historical records of benthic foraminifera could be used to reconstruct past CBA and determine the age of the first cable bacteria occurrence in the studied environments. A multivariate approach coupling the identification of lipid biomarkers in cable bacteria or eDNA, the study of foraminiferal species assemblages (C/T ratio), test preservation and isotopic test composition and the characterisation of the paleoenvironment by sedimentology and sediment geochemistry could allow us to distinguish the bacterial activity

from other factors responsible for test dissolution. Therefore, associating it with major environmental changes through time, light could be shed on the original factors of this bacterial spreading discovered only ten years ago: have they always been present without us having the tools to detect them, or have they appeared recently and are they spreading around the world?

5 CONCLUSION

This original study suggests that sediment acidification caused by cable bacteria activity could be responsible for significant calcareous test foraminifera dissolution patterns. As a result, proportions of calcareous test would change in both living and dead assemblages. The proportion of fully dissolved tests showing only their organic linings would increase in the living assemblages in the suboxic and anoxic zones of the sediment, as well as in the thanatocoenosis. In order to better understand this cause-and-effect relationship and reduce the uncertainty factors raised here, further *in situ* studies would need to be carried out in further locations over different periods, especially including the carbonate system. Laboratory incubation experiments would provide also a better understanding of the potential impact of this bacterial activity on the resilience of foraminiferal communities. It should allow us to learn more about the integration of their response in the historic record. Based on these hypotheses, we are entitled to ask what implications they might have for environmental interpretations of data from foraminifera use as paleoproxies, or bioindicators Eventually, we could be able to provide a historical retrospective on the presence of cable bacteria in marine sediments and their impact on the carbonate system and benthic meiofauna.

Data availability. All of the data are published within this paper and in the Supplement. The raw data used to make the figures are available on request.

Author contributions. Maxime DAVIRAY (foraminiferal and geochemical analysis, writing, review and editing), Emmanuelle GESLIN (head of CB-For CNRS project, foraminiferal analysis, writing, review and editing), Nils RISGAARD-PETERSEN (statistical inference, writing, review and editing), Vincent SCHOLZ (qPCR proceeding, review and editing), Marie FOUET (field work, review and editing), Edouard METZGER (microprofile acquisition, writing, review and editing).

Competing interests. At least one of the (co-)authors is a member of the editorial board of Biogeosciences.

Acknowledgments. The authors are grateful to Sophie QUINCHARD for assistance with the foraminifera picking, Sophie SANCHEZ for sample splitting (LPG, Université d'Angers) and Romain MALLET (SCIAM, Université d'Angers) for the achievement of a part of the SEM imaging. Susanne NIELSEN and Ian MARSHALL (Aarhus University) are thanked for assistance with the qPCR analysis. The authors are grateful to Frans JORISSEN for field work, and his advice for the writing process (LPG, Université d'Angers). The authors thank the participants to the field trips (2019 and 2020). The authors also thank Sebastiaan van de Velde and the two anonymous reviewers for their constructive comments.

Financial support. The authors received funding from the CNRS-INSU (program LEFE-CYBER, project CB-FOR), from the Angers University and from the OFB (project FORESTAT).

REFERENCES

Aller, R. C., Aller, J. Y., Zhu, Q., Heilbrun, C., Klingensmith, I., and Kaushik, A.: Worm tubes as conduits for the electrogenic microbial grid in marine sediments, Science Advances, 5, eaaw3651, https://doi.org/10.1126/sciadv.aaw3651, 2019.

Alve, E., and Nagy, J. (1986). Estuarine foraminiferal distribution in Sandebukta, a branch of the Oslo Fjord (Norway). *Journal of Foraminiferal Research - J FORAMIN RES* 16, 261–284. doi: 10.2113/gsjfr.16.4.261.

Anschutz, P., Chaillou, G., and Lecroart, P. (2007). Phosphorus diagenesis in sediment of the Thau Lagoon. *Estuarine, Coastal and Shelf Science* 72, 447–456. doi: 10.1016/j.ecss.2006.11.012.

Balsamo, M., Semprucci, F., Frontalini, F., and Coccioni, R. (2012). "Meiofauna as a Tool for Marine Ecosystem Biomonitoring," in *Marine ecosystems* (InTech), 77–104.

Bentov, S., Brownlee, C., and Erez, J. (2009). The role of seawater endocytosis in the biomineralization process in calcareous foraminifera. *Proceedings of the National Academy of Sciences* 106, 21500–21504. doi: 10.1073/pnas.0906636106.

Bernhard, J. M., and Bowser, S. S. (1996). Novel epifluorescence microscopy method to determine life position of foraminifera in sediments. *J. Micropalaeontol.* 15, 68–68. doi: 10.1144/jm.15.1.68.

Bernhard, J. M., Ostermann, D. R., Williams, D. S., and Blanks, J. K. (2006). Comparison of two methods to identify live benthic foraminifera: A test between Rose Bengal and CellTracker Green with implications for stable isotope paleoreconstructions: Foraminifera Viability Method Comparison. *Paleoceanography* 21. doi: 10.1029/2006PA001290.

Boudagher-Fadel, M. K. (2018). "Biology and Evolutionary History of Larger Benthic Foraminifera," in *Evolution and Geological Significance of Larger Benthic Foraminifera* (UCL Press), 1–44. doi: 10.2307/j.ctvqhsq3.3.

Burdorf, L. D. W., Tramper, A., Seitaj, D., Meire, L., Hidalgo-Martinez, S., Zetsche, E.-M., et al. (2017). Long-distance electron transport occurs globally in marine sediments. *Biogeosciences* 14, 683–701. doi: 10.5194/bg-14-683-2017.

Buzas-Stephens, P. (2005). Population Dynamics and Dissolution of Foraminifera in Nueces Bay, Texas. *The Journal of Foraminiferal Research* 35, 248–258. doi: 10.2113/35.3.248.

Cesbron, F., Metzger, E., Launeau, P., Deflandre, B., Delgard, M.-L., Thibault de Chanvalon, A., et al. (2014). Simultaneous 2D Imaging of Dissolved Iron and Reactive Phosphorus in Sediment Porewaters by Thin-Film and Hyperspectral Methods. *Environ. Sci. Technol.* 48, 2816–2826. doi: 10.1021/es404724r.

Cesbron, F., Geslin, E., Jorissen, F. J., Delgard, M. L., Charrieau, L., Deflandre, B., et al. (2016). Vertical distribution and respiration rates of benthic foraminifera: Contribution to aerobic remineralization in intertidal mudflats covered by *Zostera noltei* meadows. *Estuarine, Coastal and Shelf Science* 179, 23–38. doi: 10.1016/j.ecss.2015.12.005.

Charrieau, L. M., Bryngemark, L., Hansson, I., and Filipsson, H. L. (2018a). Improved wet splitter for micropalaeontological analysis, and assessment of uncertainty using data from splitters. *J. Micropalaeontol.* 37, 191–194. doi: 10.5194/jm-37-191-2018.

Charrieau, L. M., Filipsson, H. L., Ljung, K., Chierici, M., Knudsen, K. L., and Kritzberg, E. (2018b). The effects of multiple stressors on the distribution of coastal benthic foraminifera: A case study from the Skagerrak-Baltic Sea region. *Marine Micropaleontology* 139, 42–56. doi: 10.1016/j.marmicro.2017.11.004.

Charrieau, L. M., Filipsson, H. L., Nagai, Y., Kawada, S., Ljung, K., Kritzberg, E., et al. (2018c). Decalcification and survival of benthic foraminifera under the combined impacts of varying pH and salinity. *Marine Environmental Research* 138, 36–45. doi: 10.1016/j.marenvres.2018.03.015.

Charrieau, L. M., Nagai, Y., Kimoto, K., Dissard, D., Below, B., Fujita, K., and Toyofuku, T.: The coral reef-dwelling Peneroplis spp. shows calcification recovery to ocean acidification conditions, Sci Rep, 12, 6373, https://doi.org/10.1038/s41598-022-10375-w, 2022.

Choquel, C., Geslin, E., Metzger, E., Filipsson, H. L., Risgaard-Petersen, N., Launeau, P., et al. (2021). Denitrification by benthic foraminifera and their contribution to N-loss from a fjord environment. *Biogeosciences* 18, 327–341. doi: 10.5194/bg-18-327-2021.

Corliss, B. H., and Honjo, S. (1981). Dissolution of Deep-Sea Benthonic Foraminifera. *Micropaleontology* 27, 356. doi: 10.2307/1485191.

de Nooijer, L. J., Toyofuku, T., and Kitazato, H. (2009). Foraminifera promote calcification by elevating their intracellular pH. *Proceedings of the National Academy of Sciences* 106, 15374–15378. doi: 10.1073/pnas.0904306106.

de Nooijer, L. J., Spero, H. J., Erez, J., Bijma, J., and Reichart, G. J. (2014). Biomineralization in perforate foraminifera. *Earth-Science Reviews* 135, 48–58. doi: 10.1016/j.earscirev.2014.03.013.

Debenay, J.-P., Guillou, J.-J., Redois, F., and Geslin, E. (2000). “Distribution Trends of Foraminiferal Assemblages in Paralic Environments,” in *Environmental Micropaleontology: The Application of Microfossils to Environmental Geology* Topics in Geobiology., ed. R. E. Martin (Boston, MA: Springer US), 39–67. doi: 10.1007/978-1-4615-4167-7_3.

Debenay, J.-P., Bicchi, E., Goubert, E., and Armynot du Châtelet, E. (2006). Spatio-temporal distribution of benthic foraminifera in relation to estuarine dynamics (Vie estuary, Vendée, W France). *Estuarine, Coastal and Shelf Science* 67, 181–197. doi: 10.1016/j.ecss.2005.11.014.

Delgard, M. L., Deflandre, B., Kochoni, E., Avaro, J., Cesbron, F., Bichon, S., et al. (2016). Biogeochemistry of dissolved inorganic carbon and nutrients in seagrass (Zostera noltei) sediments at high and low biomass. *Estuarine, Coastal and Shelf Science* 179, 12–22. doi: 10.1016/j.ecss.2016.01.012.

Durand, M., Mojtahid, M., Maillet, G. M., Baltzer, A., Schmidt, S., Blet, S., et al. (2018). Late Holocene record from a Loire River incised paleovalley (French inner continental shelf): Insights into regional and global forcing factors. *Palaeogeography, Palaeoclimatology, Palaeoecology* 511, 12–28. doi: 10.1016/j.palaeo.2018.06.035.

Envlit Bassin Loire-Bretagne. Available online: https://wwz.ifremer.fr/envlit/DCE/La-DCE-par-bassin/Bassin-Loire-Bretagne (accessed on 29 Novembre 2023).

Fouet, M. P. A., Singer, D., Coynel, A., Héliot, S., Howa, H., Lalande, J., et al. (2022). Foraminiferal Distribution in Two Estuarine Intertidal Mudflats of the French Atlantic Coast: Testing the Marine Influence Index. *Water* 14, 645. doi: 10.3390/w14040645.

Fouet, M.: Répartition des communautés de foraminifères dans les estuaires de la façade atlantique, Thèse de doctorat, Université d'Angers, Université d'Angers, 270 pp., 2022.

Geelhoed, J. S., van de Velde, S. J., and Meysman, F. J. R. (2020). Quantification of Cable Bacteria in Marine Sediments via qPCR. *Frontiers in Microbiology* 11, 1506. doi: 10.3389/fmicb.2020.01506.

Geslin, E., Heinz, P., Jorissen, F., and Hemleben, Ch. (2004). Migratory responses of deep-sea benthic foraminifera to variable oxygen conditions: laboratory investigations. *Marine Micropaleontology* 53, 227–243. doi: 10.1016/j.marmicro.2004.05.010.

Gonzales, M. V., De Almeida, F. K., Costa, K. B., Santarosa, A. C. A., Camillo, E., De Quadros, J. P., et al. (2017). Helpd Index: *Hoeglundina elegans* Preservation Index for Marine Sediments in the Western South Atlantic. *Journal of Foraminiferal Research* 47, 56–69. doi: 10.2113/gsjfr.47.1.56.

Hansen, H. J. (1999). "Shell construction in modern calcareous Foraminifera," in *Modern Foraminifera* (Dordrecht: Springer Netherlands), 57–70. doi: 10.1007/0-306-48104-9_4.

Haynert, K., Schönfeld, J., Riebesell, U., and Polovodova, I. (2011). Biometry and dissolution features of the benthic foraminifer Ammonia aomoriensis at high pCO_2. *Marine Ecology Progress Series* 432, 53–67. doi: 10.3354/meps09138.

Haynert, K., Schönfeld, J., Polovodova-Asteman, I., and Thomsen, J. (2012). The benthic foraminiferal community in a naturally CO_2-rich coastal habitat of the southwestern Baltic Sea. *Biogeosciences* 9, 4421–4440. doi: 10.5194/bg-9-4421-2012.

Haynert, K., Schönfeld, J., Schiebel, R., Wilson, B., and Thomsen, J. (2014). Response of benthic foraminifera to ocean acidification in their natural sediment environment: a long-term culturing experiment. *Biogeosciences* 11, 1581–1597. doi: 10.5194/bg-11-1581-2014.

Haynes, J. R. (1981). *Foraminifera*. Springer.

Hermans, M., Lenstra, W. K., Hidalgo-Martinez, S., van Helmond, N. A. G. M., Witbaard, R., Meysman, F. J. R., et al. (2019). Abundance and Biogeochemical Impact of Cable Bacteria in Baltic Sea Sediments. *Environ. Sci. Technol.* 53, 7494–7503. doi: 10.1021/acs.est.9b01665.

Hess, S., Alve, E., Trannum, H. C., and Norling, K. (2013). Benthic foraminiferal responses to water-based drill cuttings and natural sediment burial: Results from a mesocosm experiment. *Marine Micropaleontology* 101, 1–9. doi: 10.1016/j.marmicro.2013.03.004.

Jorissen, F. J., Fouet, M. P. A., Singer, D., and Howa, H. (2022). The Marine Influence Index (MII): A Tool to Assess Estuarine Intertidal Mudflat Environments for the Purpose of Foraminiferal Biomonitoring. *Water* 14, 676. doi: 10.3390/w14040676.

Jorissen, F. J., Fouet, M. P. A., Armynot du Châtelet, E., Barras, C., Bouchet, V. M. P., Daviray, M., et al. (2023). *Foraminifères estuariens de la façade atlantique française - Guide de détermination*. Université d'Angers; OFB.

Kassambara A (2022). _rstatix: Pipe-Friendly Framework for Basic Statistical Tests_. R package version 0.7.1, https://CRAN.R-project.org/package=rstatix.

Katz, M. E., Cramer, B. S., Franzese, A., Hönisch, B., Miller, K. G., Rosenthal, Y., et al. (2010). Traditional and Emerging Geochemical Proxies in Foraminifera. *Journal of Foraminiferal Research* 40, 165–192. doi: 10.2113/gsjfr.40.2.165.

Keul, N., Langer, G., Thoms, S., de Nooijer, L. J., Reichart, G.-J., and Bijma, J. (2017). Exploring foraminiferal Sr/Ca as a new carbonate system proxy. *Geochimica et Cosmochimica Acta* 202, 374–386. doi: 10.1016/j.gca.2016.11.022.

Koho, K. A., Piña-Ochoa, E., Geslin, E., and Risgaard-Petersen, N. (2011). Vertical migration, nitrate uptake and denitrification: survival mechanisms of foraminifers (Globobulimina turgida) under low oxygen conditions: Survival mechanisms of foraminifers. *FEMS Microbiology Ecology* 75, 273–283. doi: 10.1111/j.1574-6941.2010.01010.x.

Kurtarkar, S. R., Nigam, R., Saraswat, R., and Linshy, V. N. (2011). Regenaration and Abnormality in Benthic Foraminiefra *Rosalina leei*: Implications in Reconstructing Past Salinity Changes. *Rivista Italiana Di Paleontologia e Stratigrafia*, 189-196.

Langlet, D., Geslin, E., Baal, C., Metzger, E., Lejzerowicz, F., Riedel, B., et al. (2013). Foraminiferal survival after long-term *in situ* experimentally induced anoxia. *Biogeosciences* 10, 7463–7480. doi: 10.5194/bg-10-7463-2013.

Langlet, D., Baal, C., Geslin, E., Metzger, E., Zuschin, M., Riedel, B., et al. (2014). Foraminiferal species responses to in situ, experimentally induced anoxia in the Adriatic Sea. *Biogeosciences* 11, 1775–1797. doi: 10.5194/bg-11-1775-2014.

Le Cadre, V. (2003). Low pH Effects on *Ammonia becarii* Test Deformation: Implications for Using Test deformations as a Pollution Indicator. *The Journal of Foraminiferal Research* 33, 1–9. doi: 10.2113/0330001.

Lipsewers, Y. A., Vasquez-Cardenas, D., Seitaj, D., Schauer, R., Hidalgo-Martinez, S., Sinninghe Damsté, J. S., et al. (2017). Impact of Seasonal Hypoxia on Activity and Community Structure of Chemolithoautotrophic Bacteria in a Coastal Sediment. *Appl Environ Microbiol* 83. doi: 10.1128/AEM.03517-16.

Malkin, S. Y., Rao, A. M., Seitaj, D., Vasquez-Cardenas, D., Zetsche, E.-M., Hidalgo-Martinez, S., et al. (2014). Natural occurrence of microbial sulphur oxidation by long-range electron transport in the seafloor. *ISME J* 8, 1843–1854. doi: 10.1038/ismej.2014.41.

Malkin, S. Y., Seitaj, D., Burdorf, L. D. W., Nieuwhof, S., Hidalgo-Martinez, S., Tramper, A., et al. (2017). Electrogenic Sulfur Oxidation by Cable Bacteria in Bivalve Reef Sediments. *Front. Mar. Sci.* 4. doi: 10.3389/fmars.2017.00028.

Malkin, S. Y., Liau, P., Kim, C., Hantsoo, K. G., Gomes, M. L., and Song, B. (2022). Contrasting controls on seasonal and spatial distribution of marine cable bacteria (*Candidatus* Electrothrix) and *Beggiatoaceae* in seasonally hypoxic Chesapeake Bay. *Limnology and Oceanography* 67, 1357–1373. doi: 10.1002/lno.12087.

Martin, R. E. (2000). *Environmental Micropaleontology: The Application of Microfossils to Environmental Geology*. Kluwer Academic/Plenum Publishers. Springer Available at: https://doi.org/10.1007/978-1-4615-4167-7.

Marzocchi, U., Trojan, D., Larsen, S., Louise Meyer, R., Peter Revsbech, N., Schramm, A., et al. (2014). Electric coupling between distant nitrate reduction and sulfide oxidation in marine sediment. *ISME J* 8, 1682–1690. doi: 10.1038/ismej.2014.19.

McIntyre-Wressnig, A., Bernhard, J. M., Wit, J. C., and Mccorkle, D. C.: Ocean acidification not likely to affect the survival and fitness of two temperate benthic foraminifera species: results from culture experiements, Journal of Foraminiferal Research, 44, 341–351, https://doi.org/10.2113/gsjfr.44.4.341, 2014.

Menier, D. and Dubois, A.: Carte 7137G Natures de fond du Golfe du Morbihan à 1/20 000, Service Hydrographique & Océanographique de la Marine, (S.H.O.M), 2011.

Menier, D., Tessier, B., Dubois, A., Goubert, E., and Sedrati, M.: Geomorphological and hydrodynamic forcing of sedimentary bedforms - Example of Gulf of Morbihan (South Brittany, Bay of Biscay), Journal of Coastal Research, 1530–1534, 2011.

Metzger, E., Simonucci, C., Viollier, E., Sarazin, G., Prévot, F., and Jézéquel, D. (2007). Benthic response to shellfish farming in Thau lagoon: Pore water signature. *Estuarine, Coastal and Shelf Science* 72, 406–419. doi: 10.1016/j.ecss.2006.11.011.

Meysman, F. J. R., Risgaard-Petersen, N., Malkin, S. Y., and Nielsen, L. P. (2015). The geochemical fingerprint of microbial long-distance electron transport in the seafloor. *Geochimica et Cosmochimica Acta* 152, 122–142. doi: 10.1016/j.gca.2014.12.014.

Michaud, E., Aller, R., Zhu, Q., Heilbrun, C., and Stora, G.: Density and size-dependent bioturbation effects of the infaunal polychaete Nephtys incisa on sediment biogeochemistry and solute exchange, Journal of marine research, 79, 181, https://doi.org/10.1357/002224021834670801, 2021.

Middelburg, J. J., Soetaert, K., and Hagens, M.: Ocean Alkalinity, Buffering and Biogeochemical Processes, Reviews of Geophysics, 58, e2019RG000681, https://doi.org/10.1029/2019RG000681, 2020.

Mojtahid, M., Depuydt, P., Mouret, A., Le Houedec, S., Fiorini, S., Chollet, S., Massol, F., Dohou, F., Filipsson, H. L., Boer, W., Reichart, G.-J., and Barras, C.: Assessing the impact of different carbonate system parameters on benthic foraminifera from controlled growth experiments, Chemical Geology, 623, 121396, https://doi.org/10.1016/j.chemgeo.2023.121396, 2023.

Murray, J. W. (2006). *Ecology and Applications of Benthic Foraminifera*. Cambridge University Press.

Nielsen, L. P., Risgaard-Petersen, N., Fossing, H., Christensen, P. B., and Sayama, M. (2010). Electric currents couple spatially separated biogeochemical processes in marine sediment. *Nature* 463, 1071–1074. doi: 10.1038/nature08790.

O'Brien, P. A. J., Polovodova Asteman, I., and Bouchet, V. M. P. (2021). Benthic Foraminiferal Indices and Environmental Quality Assessment of Transitional Waters: A Review of Current Challenges and Future Research Perspectives. *Water* 13, 1898. doi: 10.3390/w13141898.

Office Français De La Biodiversité Découvrir Les Estuaires de La Façade Manche/Atlantique | Le Portail Technique De l'OFB. Available online: https://professionnels.ofb.fr/fr/node/276 (accessed on 29 Novembre 2023).

Patterson, R. T., and Fishbein, E. (1989). Re-examination of the statistical methods used to determine the number of point counts needed for micropaleontological quantitative research. *J. Paleontol.* 63, 245–248. doi: 10.1017/S0022336000019272.

Petersen, J., Barras, C., Bézos, A., La, C., de Nooijer, L. J., Meysman, F. J. R., Mouret, A., Slomp, C. P., and Jorissen, F. J.: Mn/Ca intra- and inter-test variability in the benthic foraminifer

Ammonia tepida, Biogeosciences, 15, 331–348, https://doi.org/10.5194/bg-15-331-2018, 2018.

Pfeffer, C., Larsen, S., Song, J., Dong, M., Besenbacher, F., Meyer, R. L., et al. (2012). Filamentous bacteria transport electrons over centimetre distances. *Nature* 491, 218–221. doi: 10.1038/nature11586.

Polovodova, I., and Schonfeld, J. (2008). Foraminiferal Test Abnormalities in the Western Baltic Sea. *The Journal of Foraminiferal Research* 38, 318–336. doi: 10.2113/gsjfr.38.4.318.

Pucci, F., Geslin, E., Barras, C., Morigi, C., Sabbatini, A., Negri, A., et al. (2009). Survival of benthic foraminifera under hypoxic conditions: Results of an experimental study using the CellTracker Green method. *Marine Pollution Bulletin* 59, 336–351. doi: 10.1016/j.marpolbul.2009.08.015.

R Core Team (2022). R: A language and environment for statistical computing. R Foundation for Statistical Computing, Vienna, Austria. URL https://www.R-project.org/

Rao, A. M. F., Malkin, S. Y., Hidalgo-Martinez, S., and Meysman, F. J. R. (2016). The impact of electrogenic sulfide oxidation on elemental cycling and solute fluxes in coastal sediment. *Geochimica et Cosmochimica Acta* 172, 265–286. doi: 10.1016/j.gca.2015.09.014.

Réseau SYVEL Système de veille dans l'estuaire de la Loire GIP Loire Estuaire, https://www.loire-estuaire.org/dif/do/init (assessed on 29 Novembre 2023)

Revsbech, N. P., and Jørgensen, B. B. (1986). “Microelectrodes: Their Use in Microbial Ecology,” in *Advances in Microbial Ecology* Advances in Microbial Ecology., ed. K. C. Marshall (Boston, MA: Springer US), 293–352. doi: 10.1007/978-1-4757-0611-6_7.

Revsbech, N. P. (1989). An oxygen microsensor with a guard cathode. *Limnol. Oceanogr.* 34, 474–478. doi: 10.4319/lo.1989.34.2.0474.

Richirt, J., Guihéneuf, A., Mouret, A., Schweizer, M., Slomp, C. P., and Jorissen, F. J. (2022). A historical record of benthic foraminifera in seasonally anoxic Lake Grevelingen, the Netherlands. *Palaeogeography, Palaeoclimatology, Palaeoecology* 599, 111057. doi: 10.1016/j.palaeo.2022.111057.

Risgaard-Petersen, N., Revil, A., Meister, P., and Nielsen, L. P. (2012). Sulfur, iron-, and calcium cycling associated with natural electric currents running through marine sediment. *Geochimica et Cosmochimica Acta* 92, 1–13. doi: 10.1016/j.gca.2012.05.036.

Risgaard-Petersen, N., Damgaard, L. R., Revil, A., and Nielsen, L. P. (2014). Mapping electron sources and sinks in a marine biogeobattery. *Journal of Geophysical Research: Biogeosciences* 119, 1475–1486. doi: 10.1002/2014JG002673.

Risgaard-Petersen, N., Kristiansen, M., Frederiksen, R. B., Dittmer, A. L., Bjerg, J. T., Trojan, D., et al. (2015). Cable Bacteria in Freshwater Sediments. *Appl Environ Microbiol* 81, 6003–6011. doi: 10.1128/AEM.01064-15.

Schönfeld, J., and Mendes, I. (2022). Benthic foraminifera and pore water carbonate chemistry on a tidal flat and salt marsh at Ria Formosa, Algarve, Portugal. *Estuarine, Coastal and Shelf Science* 276, 108003. doi: 10.1016/j.ecss.2022.108003.

Scott, D. B., Medioli, F. S., and Schafer, C. T.: Monitoring in Coastal Environments Using Foraminifera and Thecamoebian Indicators, Cambridge University Press, 193 pp., 2007.

Seitaj, D., Schauer, R., Sulu-Gambari, F., Hidalgo-Martinez, S., Malkin, S. Y., Burdorf, L. D. W., et al. (2015). Cable bacteria generate a firewall against euxinia in seasonally hypoxic basins. *Proc Natl Acad Sci USA* 112, 13278–13283. doi: 10.1073/pnas.1510152112.

Soetaert, K., Hofmann, A. F., Middelburg, J. J., Meysman, F. J. R., and Greenwood, J. (2007). The effect of biogeochemical processes on pH. *Marine Chemistry* 105, 30–51. doi: 10.1016/j.marchem.2006.12.012.

Thibault de Chanvalon, A., Metzger, E., Mouret, A., Cesbron, F., Knoery, J., Rozuel, E., et al. (2015). Two-dimensional distribution of living benthic foraminifera in anoxic sediment layers of an estuarine mudflat (Loire Estuary, France). Biogeochemistry: Sediment doi: 10.5194/bgd-12-10311-2015.

Thibault de Chanvalon, A., Metzger, E., Mouret, A., Knoery, J., Chiffoleau, J.-F., and Brach-Papa, C. (2016a). Particles transformation in estuaries: Fe, Mn and REE signatures through the Loire Estuary. *Journal of Sea Research* 118, 103–112. doi: 10.1016/j.seares.2016.11.004.

Thibault de Chanvalon, A., Mouret, A., Knoery, J., Geslin, E., Péron, O., and Metzger, E. (2016b). Manganese, iron and phosphorus cycling in an estuarine mudflat, Loire, France. *Journal of Sea Research* 118, 92–102. doi: 10.1016/j.seares.2016.10.004.

Thibault de Chanvalon, A., Metzger, E., Mouret, A., Knoery, J., Geslin, E., and Meysman, F. J. R. (2017). Two dimensional mapping of iron release in marine sediments at submillimetre scale. *Marine Chemistry* 191, 34–49. doi: 10.1016/j.marchem.2016.04.003.

Thibault de Chanvalon, A., Geslin, E., Mojtahid, M., Métais, I., Méléder, V., and Metzger, E. (2022). Multiscale analysis of living benthic foraminiferal heterogeneity: Ecological advances from an intertidal mudflat (Loire estuary, France). *Continental Shelf Research* 232, 104627. doi: 10.1016/j.csr.2021.104627.

Toyofuku, T., Matsuo, M. Y., de Nooijer, L. J., Nagai, Y., Kawada, S., Fujita, K., et al. (2017). Proton pumping accompanies calcification in foraminifera. *Nat Commun* 8, 14145. doi: 10.1038/ncomms14145.

van Cappellen, P., and Wang, Y. (1996). Cycling of iron and manganese in surface sediments: A general theory for the coupled transport and reaction of carbon, oxygen, nitrogen, sulfur, iron, and manganese. *American Journal of Science* 296, 197–243.

van de Velde, S., Lesven, L., Burdorf, L. D. W., Hidalgo-Martinez, S., Geelhoed, J. S., Van Rijswijk, P., et al. (2016). The impact of electrogenic sulfur oxidation on the biogeochemistry of coastal sediments: A field study. *Geochimica et Cosmochimica Acta* 194, 211–232. doi: 10.1016/j.gca.2016.08.038.

World Register of Marine Species. Available online: https://www.marinespecies.org/index.php (assessed on 05 May 2022).

Appendix. *Foraminiferal absolute densities and ratios in the Auray estuary for the three stations.*

Depth layer	**Layer volume (cm-3)**	***Haynesina germanica***	***Ammonia* spp.**	**Elphidium spp.**	***Quinqueloculina* spp.**	***DS-5 specimen***	***Ammobaculites agglutinans***	**Other agglutinans**	**Total**	**C/T ratio**	**DS-5/C ratio**

St1	[0-2 mm]	10.6	179	113	18	2	0	23	9	344	0.91	0.00
	[2-4 mm]	10.6	42	18	6	0	0	5	7	78	0.85	0.00
	[4-6 mm]	10.6	26	4	0	0	0	3	0	33	0.91	0.00
	[6-8 mm]	10.6	28	9	1	0	0	3	0	41	0.93	0.00
	[8-10 mm]	10.6	15	5	0	0	0	3	2	25	0.80	0.00
	[10-12 mm]	10.6	26	5	0	0	0	4	4	39	0.79	0.00
	[12-14 mm]	10.6	23	1	0	0	0	4	2	30	0.80	0.00
	[14-16 mm]	10.6	15	5	0	0	0	4	1	25	0.80	0.00
	[16-18 mm]	10.6	25	3	1	0	0	9	2	40	0.73	0.00
	[18-20 mm]	10.6	12	4	1	0	0	3	0	20	0.85	0.00
	[20-30 mm]	52.8	110	61	2	0	0	77	6	256	0.68	0.00
	[30-40 mm]	52.8	99	67	11	0	2	57	9	245	0.73	0.01
	[40-50 mm]	52.8	93	42	2	0	0	28	4	169	0.81	0.00
St2	[0-2 mm]	10.6	95	37	9	3	1	4	0	149	0.97	0.01
	[2-4 mm]	10.6	38	18	1	0	2	1	1	61	0.97	0.03
	[4-6 mm]	10.6	24	8	2	0	0	5	0	39	0.87	0.00
	[6-8 mm]	10.6	4	7	0	0	2	6	1	20	0.65	0.15
	[8-10 mm]	10.6	8	0	0	0	1	3	0	12	0.75	0.11
	[10-12 mm]	10.6	6	0	0	0	1	7	3	17	0.41	0.14
	[12-14 mm]	10.6	11	2	0	0	0	10	2	25	0.52	0.00
	[14-16 mm]	10.6	0	0	0	0	2	13	1	16	0.13	1.00
	[16-18 mm]	10.6	16	0	0	0	4	17	2	39	0.51	0.20
	[18-20 mm]	10.6	31	1	0	0	3	15	0	50	0.70	0.09
	[20-30 mm]	52.8	22	6	2	0	20	33	6	89	0.56	0.40

	[30-40 mm]	52.8	15	5	0	0	4	5	8	37	0.65	0.17
	[40-50 mm]	52.8	9	0	0	0	10	5	1	25	0.76	0.53
St 3	[0-2 mm]	10.6	238	52	19	83	0	8	5	405	0.97	0.00
	[2-4 mm]	10.6	91	11	5	8	0	7	2	124	0.93	0.00
	[4-6 mm]	10.6	148	9	4	4	2	4	2	173	0.97	0.01
	[6-8 mm]	10.6	133	4	3	1	3	6	1	151	0.95	0.02
	[8-10 mm]	10.6	73	2	2	0	2	6	1	86	0.92	0.03
	[10-12 mm]	10.6	55	2	1	0	2	1	1	62	0.97	0.03
	[12-14 mm]	10.6	60	1	2	0	3	8	1	75	0.88	0.05
	[14-16 mm]	10.6	37	6	3	0	7	3	2	58	0.91	0.13
	[16-18 mm]	10.6	21	2	0	0	5	5	2	35	0.80	0.18
	[18-20 mm]	10.6	18	4	1	0	5	5	6	39	0.72	0.18
	[20-30 mm]	52.8	38	4	0	0	21	20	16	99	0.64	0.33
	[30-40 mm]	52.8	7	4	1	0	35	15	19	81	0.58	0.74
	[40-50 mm]	52.8	8	9	1	0	57	15	32	122	0.61	0.76

888